Manufacturing of Cylindrical Micro Lenses and Micro Lens Arrays in Fused Silica and Borosilicate Glass using F_2-Laser Microstructuring

Sebastian Buettner, Michael Pfeifer and Steffen Weissmantel
Laserinstitut Hochschule Mittweida, Technikumplatz 17, Mittweida, Germany

Keywords: Cylindrical Lens, Micro Lens, Lens Array, Fused Silica, Borosilicate Glass, Fluorine Laser, Microstructuring.

Abstract: The results of our investigations on direct laser fabrication of cylindrical micro lenses and micro lens arrays in fused silica and borosilicate glass using fluorine laser microstructuring technique will be presented. The process, based on the mask projection technique, enables the generation of almost perfectly curved, smooth surfaces with a defined radius of curvature. In particular, it will be shown that one calculated mask can be used to generate different radii of curvature depending on the laser pulse fluence and the pulse-to-pulse overlap. The surface roughness of the lenses depends on the process parameters as well. To generate continuous transition areas between the lenses in one array, the optimal lens spacing was determined. Moreover, it can be shown, that the surface quality of cylindrical micro lens arrays, made of fused silica, can be improved by CO_2 laser smoothing. The minimal reached surface roughness is 4.6 nm RMS.

1 INTRODUCTION

Nowadays micro optics are becoming more and more important to deal with technical problems, e.g. in the field of data communication and beam shaping applications. A wide range of techniques was developed to manufacture optical elements in the micrometer scale in the last few years. Even the fabrication of cylindrical lenses and cylindrical lens arrays became more interesting as subject of the investigations. Many processes were developed particular for polymer materials like printing or reflow techniques (Xing et al., 2016; Huang et al., 2018; Qiu et al., 2018). Furthermore, fabrication techniques for processing fused silica, like the femtosecond (fs) laser microstructuring and a combined fs and CO_2 laser reshape technique (Luo et al., 2018; Choi et al., 2015) were developed. For processing fused silica and in particular wide band gap materials a fluorine laser can be used as well.

Based on our research in microstructuring of blaze gratings (Pfeifer, Weissmantel and Reisse, 2013), diffractive optical elements (Pfeifer et al., 2014) such as the fabrication of micro Fresnel lenses (Fricke-Begemann, Ihlemann and Wissenbach, 2006; Pfeifer et al., 2017) we further developed the fluorine laser microstructuring technique for the fabrication of cylindrical micro lenses and arrays thereof. Due to the short wavelength of the fluorine laser, wide band gap materials such as calcium fluoride as well as fused silica can be machined. The microstructuring process based on the mask projection technique. Therefore, a special mask geometry was calculated and fabricated. The use of this mask enables the fabrication of almost perfectly curved surfaces with a defined radius of curvature (ROC). In addition to the microstructuring process we further developed a laser based post-treatment process using a CO_2 laser. In this way, the surface roughness of cylindrical lenses and lens arrays made thereof can be reduced up to a few nanometers. The combination of these two laser technologies form the foundation of a new process chain for the fabrication of micro optics.

2 EXPERIMENTAL SETUP

The microstructuring is done by the laser micromachining station EX-157, which was built by 3D-Micromac AG. In this station the fluorine laser LPF 220i of Coherent (Deutschland) GmbH is integrated. The Laser beam has a wavelength of 157 nm that corresponds to a photon energy of 7.9 eV. The maximum repetition rate is 200 Hz and the pulse duration is

Buettner, S., Pfeifer, M. and Weissmantel, S.
Manufacturing of Cylindrical Micro Lenses and Micro Lens Arrays in Fused Silica and Borosilicate Glass using F2-Laser Microstructuring.
DOI: 10.5220/0007382300660072
In *Proceedings of the 7th International Conference on Photonics, Optics and Laser Technology (PHOTOPTICS 2019)*, pages 66-72
ISBN: 978-989-758-364-3

25 ns. The pulse energy can be varied from 10 to 30 mJ. Because of the wavelength in the vacuum ultraviolet (VUV) range, the beam shaping and the material processing take place in two independent vacuum chambers. The beam path can be evacuated up to a pressure of $<5 \cdot 10^{-5}$ mbar and the process chamber in the pre-vacuum range to ensure an oxygen-free atmosphere. After evacuation these chambers are flooded with pure nitrogen (5.0) to normal pressure. The fluorine laser microstructuring is done by mask projection technique. Here the mask geometry is optically imaged onto the substrate surface with a demagnification ration of 26.67 : 1. A laser pulse fluence up to 7 J/cm² can be reached in an area of maximal 225 x 225 µm² with a resolution of less than 1 µm. For the substrate movement a high-precision positioning system is installed in the process chamber.

For the post-treatment process the CO_2 laser SM600 of FEHA LaserTec GmbH is used. The wavelength of the laser beam is 10.6 µm and the maximum output power is 600 W. The laser beam is focused by a lens with a focal length of 500 mm and deflected by a scanner.

3 EXPERIMENTAL PROCEEDING

3.1 Microstructuring of Cylindrical Lenses

The microstructuring process using an excimer laser based on the mask projection technique. By using a pulsed laser system, every laser pulse remove a certain amount of material depending on the laser and material parameters. Due to the homogenization of the laser beam the laser pulse fluence H is equal all over the mask area and thereby in the image plane of the imaging system too. Therefore the ablation depth is equal all over the ablation area, which is formed by the mask geometry. In general, the depth of the microstructures depends on the laser pulse fluence and the number of pulses N per area.

The fabrication of three dimensional microstructures like cylindrical lenses requires the control of the microstructuring depth within the ablation area. This can be realized by influence the number of pulses per area. In consideration of a constant pulse-to-pulse distance the number of pulses per area can be controlled by varying the mask aperture in feed direction. The ratio of the maximum aperture and its overlap regarding to the following pulse, can be described as the pulse-to-pulse overlap. A high overlap of 90 to 99 % lead to very small areas with an equal number of pulses. Therefore, the course of the surface is almost continuous. As described, the number of laser pulses per area depend on the mask aperture. Due to this, the course of the mask aperture has to be proportional to the course of the depth h(r), referred to the vertex of the lens. It could be described as a part of a circular sector as shown in Figure 1.

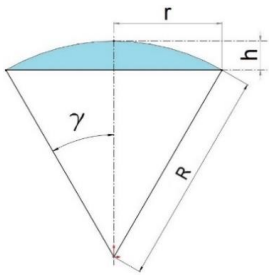

Figure 1: Geometric description of the lens surface by means of a circular sector and its parameters.

The depth h(r) is calculated from the radius of curvature R and the distance r according to Eq. (1). The calculated mask geometry is shown in Figure 2. For the calculation the cos-terms were used only. Due to the small values of h(r), a scaling factor was used instead of the ROC.

$$h(r) = R \cdot \left(1 - \cos\left(\sin\left(\frac{r}{R}\right)^{-1}\right)\right) \quad (1)$$

Figure 2: Calculated mask aperture for the fabrication of an 85 µm width cylindrical lens.

3.2 Co2 Laser Smoothing

The smoothing of fused silica using a CO_2 laser was developed for the polishing of macroscopic lenses (Richmann, Willenborg and Wissenbach, 2010). We further developed this process for the smoothing of the surface of diffractive optical elements (Pfeifer, Büttner and Weissmantel, 2015). That process based on the redistribution of the material, which is effected by the surface tension of the molten material. Due to this, the surface is minimized. This corresponds to a reduction of the surface roughness. However, the process requires the heating of the material over the

softening temperature of 1,585 °C. For this a CO_2 laser is used. Because of the wavelength of 10.6 µm and the high absorption coefficient of the material, the laser radiation is absorbed in a thin layer of a few microns. A focusing lens and a scanner is used to form a focal line on the substrate surface. According to this, a temperature field is generated. During the treatment, the substrate is moved perpendicular to the scanning direction. This effects a movement of the temperature field over the substrate. To reach a defined and constant surface temperature the laser power is controlled by a pyrometer and a programmable logic controller (SPS). For this a PID-algorithm converts the temperature into a reference voltage. Moreover, a heat plate is used to pre-heat the substrate to more than 400 °C. This shall reduce thermally induced stresses during the treatment.

4 RESULTS AND DISCUSSION

4.1 Material and Process Dependencies

The microstructuring of cylindrical lenses requires the knowledge of the specific material parameters ablation threshold H_s and absorption coefficient α. For our investigations the fused silica Corning 7980 (standard grade) and the borosilicate glass Schott D263T were used. In a first step these parameters were determined using Lambert-Beer law (Table 1).

Table 1: Determined ablation threshold H_s and absorption coefficient α for Corning 7980 and Schott D263T.

Material	H_s in J/cm²	α in cm^{-1}
Corning 7980	0.56	$12.98 \cdot 10^4$
Schott D263T	0.39	$11.09 \cdot 10^4$

For each material the influence of varying the laser pulse fluence and the pulse-to-pulse overlap was studied. Figure 3 shows a set of cylindrical lenses fabricated at 3 J/cm² and different pulse-to-pulse overlaps. In general the measured values are in good agreement with the theoretical values. The microstructuring process was simulated in advance using the calculated mask geometry and the ablation parameters. The values of the ROC were calculated from the simulated surface profile as well as from the measured surface profile by a best-circular-fit algorithm. The deviations depend on fluctuations of the laser power during the lens fabrication. In particular at low laser pulse fluences and small overlaps, a change of the laser power causes a strong change of the ROC. In general the ROC degreases by increasing laser pulse fluence and pulse-to-pulse overlap, as shown in Figure 4.

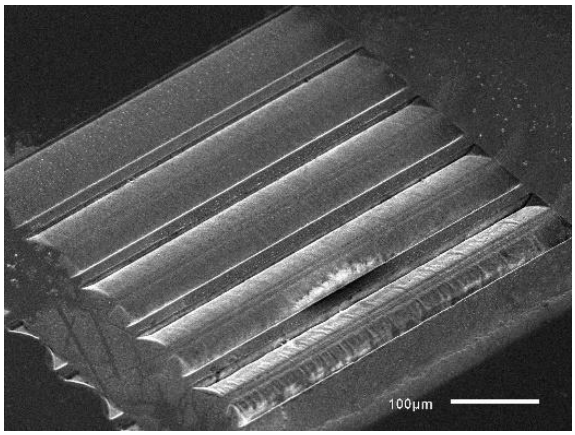

Figure 3: Scanning electron microscope (SEM) image of 85 µm width cylindrical lenses, fabricated in Corning 7980 at 3 J/cm² and 90, 95, 97, 98, and 99 % overlap (top left to bottom right).

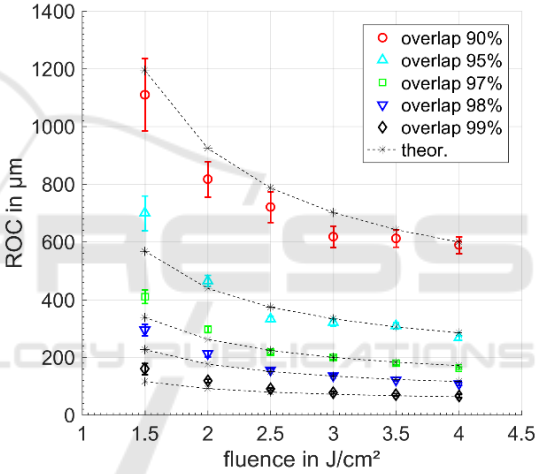

Figure 4: ROCs of the cylindrical lenses, fabricated in Corning 7980, depending on the laser pulse fluence for different overlaps.

For a higher laser pulse fluence the change of the ROC become smaller in general. The influence of the overlap can be described by a nearly linear behavior as shown in Figure 5. The ROCs of the lenses fabricated in Schott D263T behave in a similar way. Due to the lower threshold and absorption coefficient of this material the ROCs are lower in comparison to fused silica (see Figure 6).
In general the surface profile of the lenses fits almost perfectly to a circular form. A high pulse-to-pulse overlap of more than 99 % lead to a strong increase of the ablation depth per area, in particular at high fluences. As a result, the surface profile deviates from the circular form. The higher the ablation depth per pulse and the pulse-to-pulse overlap, the more the lenses become an elliptical shape.

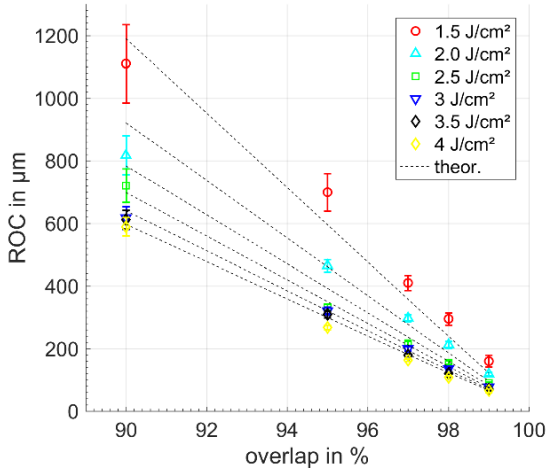

Figure 5: ROCs of the cylindrical lenses, fabricated in Corning 7980, depending on the overlap for different laser pulse fluences.

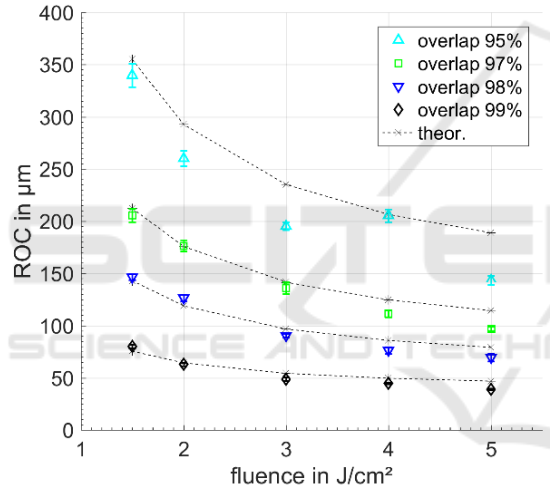

Figure 6: ROCs of the cylindrical lenses, fabricated in Schott D263T, depending on the laser pulse fluence for different overlaps.

This could have a negative effect on the optical property of the lenses. But it also can be used for a correction of the spherical aberration, in particular for lenses with a short focal length. In Addition to this, the surface roughness depend on the process parameters and in particular on the pulse-to-pulse overlap. Figure 7 and Figure 8 show the measured roughness values (RMS) of the lens surfaces. As can be seen in these figures, most of the lenses got a roughness in the range of 50 to 100 nm RMS. For an overlap of 99 % the roughness rises up to 132 nm for lenses in Corning 7980 and almost to 350 nm for lenses in Schott D263T.

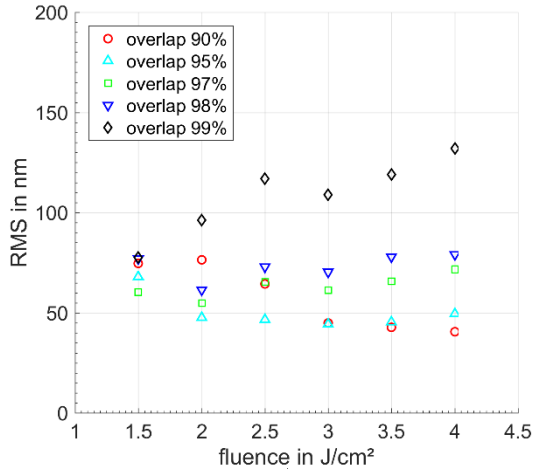

Figure 7: Measured surface roughness (RMS) of the cylindrical lenses fabricated in Corning 7980 (λ_c = 8 µm).

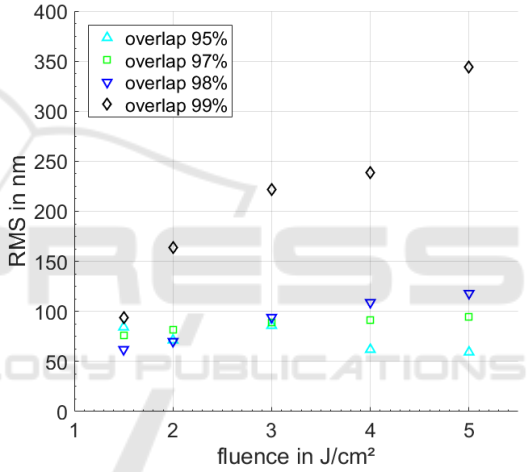

Figure 8: Measured surface roughness (RMS) of the cylindrical lenses fabricated in Schott D263T, depending on the laser pulse fluence for different overlaps (λ_c = 8 µm).

4.2 Lens Array Fabrication

The fabrication of lens arrays can be done by microstructuring of two or more lenses next to each other. Therefore, the spacing between two lenses first was set to the lens aperture of 85 µm. As a result, the material in the transition areas could not be removed completely. To optimize these areas the spacing from one single lenses to the next was reduced in steps of 1 µm from 85 µm to 75 µm. In Figure 9 a section of a surface profile of a lens array is shown. Moreover, it can be seen that the material in the transition area can be removed almost completely. The lens arrays fabricated in fused silica become smoothed using the CO_2 laser setup as described above. The lens array presented in Figure 10 was fabricated in Corning

7980 at 3 J/cm² and with a pulse-to-pulse overlap of 97 %. The initial roughness of the lens surface is 44.1 ± 2.8 nm RMS. For the post treatment the temperature was set to 1,600 °C and the feed speed to 0.5 mm/s. As a result the micro roughness could be reduced to 10.3 ± 0.6 nm RMS.

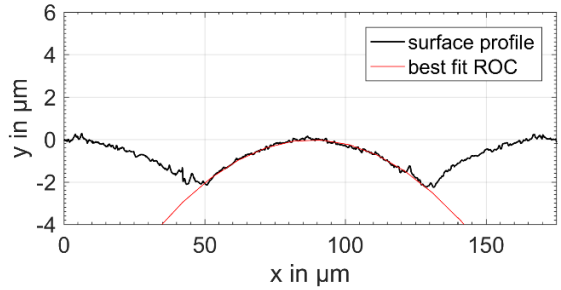

Figure 9: Surface profile of a lenses array in Corning 9780 with optimized transition areas (ROC = 374 µm, optimum spacing 81 µm).

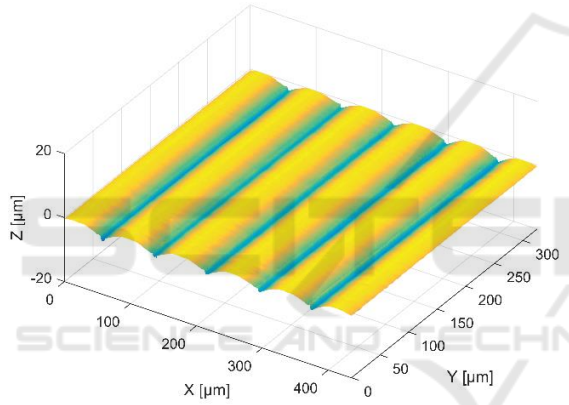

Figure 10: Confocal micrograph of a lens array fabricated in Corning 7980 (H = 3 J/cm², overlap: 97 %).

In Figure 11 the SEM-images of the lens array are shown. It can be seen, that the brightness of the lens surface is nearly equal to the untreated surface and significantly lower in comparison to the lenses shown in Figure 3. This indicates a very low micro roughness, but the images also show a slight irregular waviness at the surface of the lenses. These waviness is caused by the instability of the laser pulse energy.

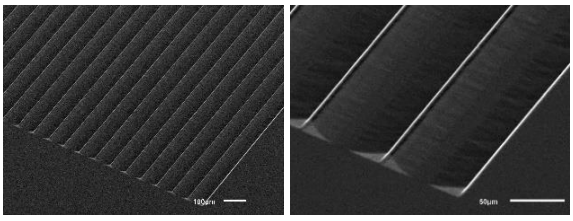

Figure 11: SEM-images of a smoothed lens array in Corning 7980 at a magnification of 100x (left) and 500x (right) (H = 3 J/cm², overlap: 97 %, T = 1,600 °C, v = 0.5 mm/s).

In general, the smoothing of the surface effects an improvement of the optical properties. This can be shown by calculating the squared electrical field strength $|E|^2$ in direction of the propagation of x. Because of the proportionality of the squared electrical field strength and the intensity, the effect of the post-treatment can be illustrated clearly. The calculations were done using the Fresnel-Kirchhoff's diffraction integral for a wavelength of 532 nm and a refractive index of 1.4607. The latter was calculated using the Sellmeier equation and the appropriate coefficients, which are given in the data sheet of Corning 7980. Moreover an electromagnetic wave with an even wave front was assumed. The phase shift, caused by a different optical thickness of the lens, was calculated using the measured surface profile. The electrical field strength was squared by element and normalized to 1 for every distance. Figure 12 shows the squared electrical field strength of a propagating electromagnetic field for a single lens of an unsmoothed and a smoothed lens array surface.

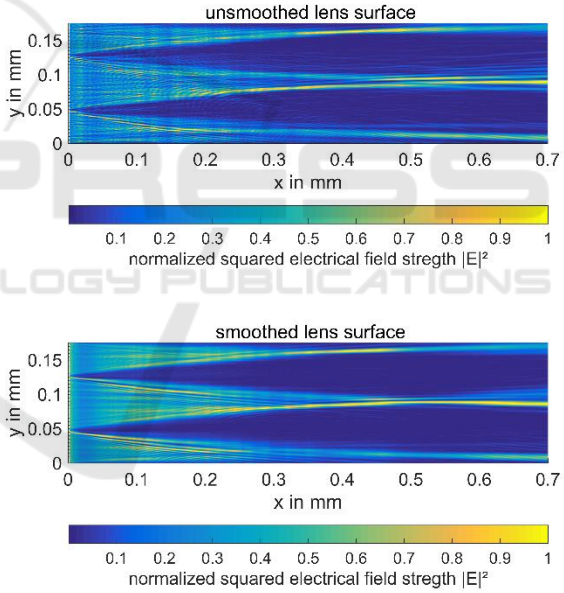

Figure 12: Squared electrical field strength $|E|^2$ normalized to 1 depending on the propagation direction x, calculated from an unsmoothed (top) and a smoothed (bottom) surface profile (λ = 532 nm, n = 1.4607).

A comparison of the two calculated distributions shows, that a smoothed lens surface focused the light better than an unsmoothed lens surface, due to a reduction of the scattering. Furthermore, it can be shown, that defects at the edge of the lenses causes an asymmetric distribution of the electric field strength. An increase of the smoothing temperature has a positive effect on the roughness and the defects at the edge

of the lenses as well. The array, shown in Figure 13, was fabricated in fused silica. The averaged ROC of the lenses is 158.2 ± 3.2 µm and the surface roughness is 79.4 nm. The lens array was smoothed at a temperature of 1,700 °C and a feed speed of 0.5 mm/s. Due to the higher temperature a surface roughness of 4.6 ± 0.8 nm could be reached. Furthermore, the defects at the edges of the lenses could be removed completely as shown in Figure 13.

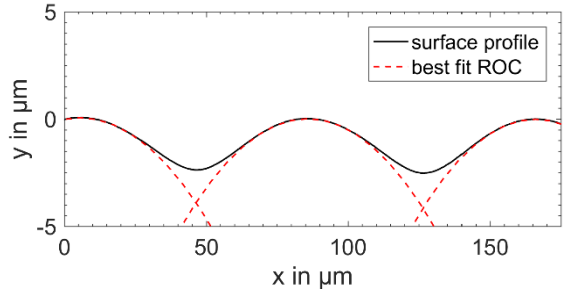

Figure 13: Surface profile of a lens array, smoothed at a temperature of T = 1,700 °C and a feed speed of v = 0.5 mm/s.

However, the higher temperature also got a negative effect on the surface profile and in particular on the transition areas and the ROC. As can be seen in the Figure 13, there is a strong deviation of the surface profile from the best fit ROC. In addition to that, the ROC increases after the smoothing due to a strong redistribution of material in general. The deviation of the surface profile from the optimum course affects the efficiency of the lens array. As can be seen in Figure 14, the transition areas do not contribute to the focusing effect of the lens areas in a right way.

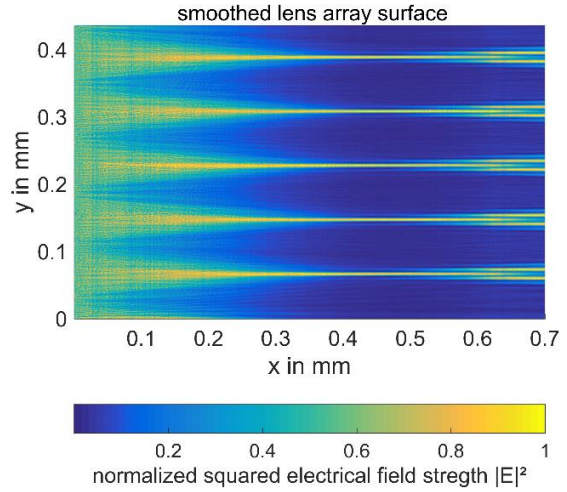

Figure 14: Squared electrical field strength $|E|^2$ normalized to 1 depending on the propagation direction x, calculated from a smoothed lens array surface profile, (T = 1,700 °C, v = 0.5 mm/s, λ = 532 nm, n = 1.4607).

But, the high smoothing temperature also lead to a symmetrical lens surface and therefore to an appropriate distribution of the electrical field strength due to the elimination of the defects at the edge of the lens surface.

5 CONCLUSIONS

The fabrication of cylindrical lenses and lens arrays in fused silica and borosilicate glass can be done by fluorine laser microstructuring using a special calculated mask. The ROCs of the cylindrical lenses depends on the laser pulse fluence and the pulse-to-pulse overlap using one calculated mask geometry. Lenses with a nearly circular surface profile and a ROC in the range of around 100 µm up to 1,200 µm can be fabricated. For a high pulse-to-pulse overlap and a high laser pulse fluence the surface profile deviates from the circular form. This could be used for the generation of aspherical shaped and particular elliptical shaped lenses with a small ROC and short focal length.

To fabricate spherical lenses with a smaller ROC, a new mask has to be designed. In general the ROC can be adjusted by the process parameters. In this regard, the process and in particular the laser power control has to be optimized to avoid the resulting waviness of the lens surface. The transition areas between the lenses of an array can be optimized by varying the spacing, in particular for larger ROCs. For smaller ROCs defects occur at the edges of the lenses, which affect the function of the lens array. Therefore, the mask geometry needs to be adapted by adding separate correction areas.

The surface roughness, which also has an influence on the function of the lenses and the arrays, can be reduced using the CO_2 laser smoothing. A minimal roughness of 4.6 ± 0.8 nm can be reached at a smoothing temperature of 1,700 °C. In general, a high smoothing temperature lead to a smooth surface. Due to this, the scattering at the lens surface can be reduced. The high smoothing temperatures also got a negative effect on the transition area and the ROC. A surface roughness of 10.3 ± 0.6 nm RMS can be reached without changing the circular lens profile.

In a next step, all of the mentioned parameters will be optimized, to reach a higher surface quality and process stability as well. The stabilization of the laser power and the pulse-to-pulse energy is the key part for increasing the quality of this laser based fabrication technique. Therefore, a fast measurement and power control system will be developed and implemented.

ACKNOWLEDGEMENTS

The authors gratefully acknowledge the financial support of the present work by the European Union and the Free State of Saxony.

REFERENCES

Xing, J., Rong, W., Sun, D., Wang, L., & Sun, L. (2016). Extrusion printing for fabrication of spherical and cylindrical microlens arrays. In Applied Optics, 55(25), pp. 6947-6952.

Huang, S., Li, M., Shen, L., Qiu, J., & Zhou, Y. (2018). Fabrication of high quality aspheric microlens array by dose-modulated lithography and surface thermal reflow. Optics & Laser Technology, 100, pp. 298-303.

Qiu, J., Li, M., Ye, H., Yang, C., & Shi, C. (2018). Fabrication of high fill factor cylindrical microlens array with isolated thermal reflow. Applied Optics, 57(25), pp. 7296-7302.

Luo, Z., Yin, K., Dong, X. & Duan, J. (2018). Fabrication of parabolic cylindrical microlens array by shaped femtosecond laser. Optical Materials, 78, pp. 465-470.

Choi, H.-K., Ahsan, M. S., Yoo, D., Sohn, I.-B., Noh, Y.-C., Kim, J.-T., Kang, H.-M. (2015). Formation of cylindrical micro-lens array on fused silica glass surface using CO_2 laser assisted reshaping technique. Optics & Laser Technology, 75, pp. 63-70.

Pfeifer, M., Weissmantel, S., Reisse, G. 2013. Direct laser fabrication of blaze gratings in fused silica. In *Applied Physics A* 112, pp. 61-64.

Pfeifer, M., Jahn, F., Kratsch, A., Steiger, B. and Weissmantel, S. 2014. F_2-Laser Microfabrication of Diffractive Optical Elements, *2nd International Conference on Photonics, Optics and Laser Technology*.

Fricke-Begemann, T., Ihlemann, J., and Meinertz, J., 2006, Diffraktive Mikrolinsen: Herstellung durch direkte Laserstrukturierung, *DGaO-Proceedings (2006).*

Pfeifer, M., Büttner, S., Zhang, R. Serbay, M. and Weissmantel, S. 2017. F2-Lasermikrostrukturieurng von Mikro-Fresnel-Linsen. In *Journal of the University of Applied Sciences Mittweida*, pp.127-130.

Richmann, A., Willenborg, E. and Wissenbach, K., 2010, Laser Polishing of Fused Silica, In *International Optical Design Conference and Optical Fabrication and Testing*.

Pfeifer, M., Büttner, S. and Weissmantel, S., 2015, CO_2-Laserglättung von diffraktiven Phasenelementen in Quarzglas, 2015, In *Journal of the University of Applied Sciences Mittweida*, pp. 187-191.